HHS Public Access

Author manuscript

Bioconjug Chem. Author manuscript; available in PMC 2016 May 03.

Published in final edited form as:

Bioconjug Chem. 2016 January 20; 27(1): 170–178. doi:10.1021/acs.bioconjchem.5b00584.

Caged [^{18}F]FDG Glycosylamines for Imaging Acidic Tumor Microenvironments Using Positron Emission Tomography

Robert R. Flavell[†], **Charles Truillet**[†], **Melanie K. Regan**[†], **Tanushree Ganguly**[†], **Joseph E. Blecha**[†], **John Kurhanewicz**[†], **Henry F. VanBrocklin**[†], **Kayvan R. Keshari**[‡], **Christopher J. Chang**[§], **Michael J. Evans**[†], and **David M. Wilson**[*,†]

[†]Department of Radiology and Biomedical Imaging, University of California, San Francisco, California 94158, United States

[‡]Department of Radiology and Molecular Pharmacology and Chemistry Program, Memorial Sloan-Kettering Cancer Center, New York, New York 10065, United States

[§]Departments of Chemistry and Molecular and Cell Biology and the Howard Hughes Medical Institute, University of California, Berkeley, California 94720, United States

Abstract

Solid tumors are hypoxic with altered metabolism, resulting in secretion of acids into the extracellular matrix and lower relative pH, a feature associated with local invasion and metastasis. Therapeutic and diagnostic agents responsive to this microenvironment may improve tumor-specific delivery. Therefore, we pursued a general strategy whereby caged small-molecule drugs or imaging agents liberate their parent compounds in regions of low interstitial pH. In this manuscript, we present a new acid-labile prodrug method based on the glycosylamine linkage, and its application to a class of positron emission tomography (PET) imaging tracers, termed [^{18}F]FDG amines. [^{18}F]FDG amines operate via a proposed two-step mechanism, in which an acid-labile precursor decomposes to form the common radiotracer 2-deoxy-2-[^{18}F]fluoro-D-glucose, which is subsequently accumulated by glucose avid cells. The rate of decomposition of [^{18}F]FDG amines is tunable in a systematic fashion, tracking the pK_a of the parent amine. In vivo, a 4-phenylbenzylamine [^{18}F]FDG amine congener showed greater relative accumulation in tumors over benign tissue, which could be attenuated upon tumor alkalinization using previously validated models, including sodium bicarbonate treatment, or overexpression of carbonic anhydrase. This new class of PET tracer represents a viable approach for imaging acidic interstitial pH with potential for clinical translation.

[*]Corresponding Author: david.m.wilson@ucsf.edu.

Author Contributions

R.R.F. and D.M.W. proposed and supervised the overall project. R.R.F. performed all synthesis and radiosynthesis. C.T. conducted the cell uptake assays. M.K.R. performed PET imaging and biodistribution experiments. T.G., J.K., K.R.K., J.E.B., H.F.V., C.J.C., and M.J.E. contributed to scientific discussion.

Notes

The authors declare no competing financial interest.

Supporting Information

The Supporting Information is available free of charge on the ACS Publications website at DOI: 10.1021/acs.bioconjchem.5b00584. Detailed methods for synthesis, in vitro assays, and biodistribution, all characterization of new compounds, and supplementary figures (PDF)

Graphical Abstract

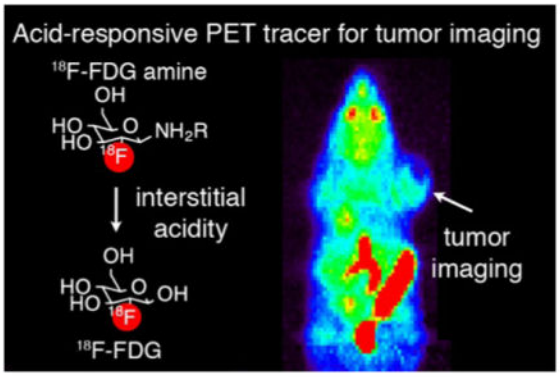

INTRODUCTION

Metabolic reprogramming in cancer is often accompanied by extracellular matrix acidification. Measurements of tumor pH, using microelectrodes, magnetic resonance, or fluorescence techniques, typically yield an extracellular pH ranging 6.5–6.9.[1–3] In contrast, normal tissues exhibit an interstitial pH ranging 7.2–7.4.[4] Importantly, acidic interstitial pH has been shown to be associated with local invasion and metastasis in a variety of tumors, including renal cell cancer, breast cancer, colon cancer, and others.[5–7] Treatment of solid tumors with sodium bicarbonate has been shown to increase tumor pH and reduce experimental metastasis.[8] Extracellular acidity has been implicated in resistance to traditional chemotherapeutic agents, and numerous small molecule agents targeting acid transporters are currently under development.[9,10] Therefore, the presence of acidic interstitium in tumors is both a potential biomarker for the presence of aggressive cancer as well as a therapeutic target.

Since acidic interstitial pH is a common pathologic feature associated with malignancies, the development of acid labile prodrugs has become an area of active research. In this general strategy, a caging group is linked to a chemotherapeutic using an acid labile bond.[11] The most commonly used acid labile bonds for this purpose include imines, hydrazones, acetals, orthoesters, and cis-aconityl linkers.[12,13] In general, the kinetics of the acid cleavage of these linkers are relatively slow, occurring over a time course of hours to days, which is optimal considering the long circulating half-life of polymer conjugates. However, in the development of acid-labile prodrugs of compounds labeled with short biological or physical (i.e., radioactive substances) half-lives, more rapid cleavage kinetics are required. This represents a particular challenge for the development of pro-drug compounds for imaging using nuclear medicine techniques such as positron emission tomography (PET), which commonly require the use of short-lived isotopes.

Several techniques, principally based on MR imaging, have been developed for the general purpose of visualizing acidic interstitial pH in vivo.[7,14,15] While these traditional techniques have yielded important insights, they are often limited by long scan time, poor spatial resolution, low signal-to-noise, and requirement for administering high doses of probe,

potentially altering systemic pH.[16–19] In comparison with these other investigational molecular imaging technologies, positron emission tomography (PET) imaging has the potential to overcome some of these limitations, owing to its relatively high spatial resolution, ability to inject tracer doses of radio-pharmaceutical, and relative ease of clinical translation. As such, there is a growing interest in PET imaging of acidic interstitial pH, and a few select elegant examples have been reported, including methods based on charge trapping of labeled radiopharmaceuticals[20–22] or pH-dependent insertion of engineered peptides into cell membranes.[23–25] Despite this progress, routine clinical translation of pH imaging remains an outstanding challenge.

With the goal of developing a pH-imaging method primed for clinical translation, we envisioned a pro-drug strategy for targeting acidic interstitial pH using PET, as we have successfully exploited this design concept in our laboratories for sensing extracellular H_2O_2 in rapidly proliferating cells.[26,27] In the present strategy, a caged derivative of a clinically utilized PET tracer is prepared, which is selectively degraded to the parent compound upon exposure to acid and can be taken up by adjacent cells. For the tracer component, we chose 2-deoxy-2-[^{18}F]fluoro-D-glucose ([^{18}F]FDG), as it is the most commonly used PET radiotracer and is used for staging and restaging of cancers in routine clinical practice.[28] [^{18}F]FDG exhibits high uptake in a wide range of cancers, as well as in other tissues with high glycolytic activity, such as brain, heart, liver, and other organs. The mechanism of uptake of [^{18}F]FDG is via glucose transporters (GLUT), with subsequent phosphorylation by hexokinase.[11] Due to its widespread availability and favorable pharmacokinetics, [^{18}F]FDG has been used to label other tracers via stable linkages.[29–39]

In this report, we describe a new strategy of acid labile prodrugs based on the glycosylamine linkage. Their rate of cleavage is tunable based on the pK_a of the parent amine, with rapid derivatives allowing application to imaging using PET. Specifically, we describe a family of acid labile prodrug [^{18}F]FDG derivatives, termed [^{18}F]FDG amines, and their in vitro and in vivo application for sensing the acidic interstitial microenvironment. This tunable, general prodrug strategy could find application outside of imaging. Furthermore, with the combination of straightforward design and synthesis methodology coupled to the widespread availability of [^{18}F]FDG, we anticipate that this approach should find value in the study of acidic interstitial pH with potential for clinical translation.

RESULTS

Tracer Design

Like glucose, [^{18}F]FDG is a reducing sugar, which is in equilibrium with its linear form that contains a unique aldehyde at its 1 position. This position was targeted for caging with an acid labile protecting group (Figure 1). Since ^{18}F has a half-life of 110 min, a rapid degradation reaction is required for this application. In initial studies, the conjugation of [^{18}F]FDG with aryl and benzoyl hydrazine derivatives was examined. We found that the hydrazone formed with benzoyl hydrazine was too stable, with no degradation apparent at pH 6.5 or 7.4 at 1 h, concordant with previous studies of glucose hydrazone stability.[40] Furthermore, aryl hydrazone derivatives could not be isolated due to rapid defluorination (SI Table 1). These results indicated that [^{18}F]FDG hydrazones would be unlikely to be useful

prodrugs for imaging the mildly acidic microenvironment seen in solid tumors (typical pH 6.5–7.0).

We next examined glycosylamines of [^{18}F]FDG, inspired by prior studies that demonstrated striking acceleration of the rate of hydrolysis of glucosylamines at mildly acidic pH.[41–44] Remarkably, despite the well-known acid lability of these compounds, they have not been previously applied to prodrug development. This is likely because glycosylamines of sugars such as glucose, with a hydroxyl group at the 2 position, can undergo the Amadori rearrangement to generate a variety of products.[45] In contrast, [^{18}F]FDG has a fluorine atom at the 2 position and cannot undergo rearrangement.[39] Therefore, [^{18}F]FDG represents an optimal model system for the development of this strategy. Hydrolysis reactions of glycosylamines proceed via an acyclic imine intermediate under general acid catalysis.[46] Imines have been used to generate acid labile prodrugs.[12] Thus, we anticipated that glycosylamines could act as an imine prodrug equivalent. Baranwal et al. recently synthesized two [^{18}F]fluorodeoxyglycosylamines, although the acid stability of these compounds was not investigated.[39] Taken together, these prior reports indicated that these [^{18}F]-fluorodeoxyglycosylamines, termed [^{18}F]FDG amines, should be synthetically accessible and yield caged [^{18}F]FDG precursors with the appropriate rapid hydrolysis.

Synthesis of [^{19}F]FDG Amine and FDG Oxime Standards

Synthesis of reference nonradioactive standards was accomplished in one step by incubation of [^{19}F]FDG with the amine in the presence of acetic acid for 1 h at 60 °C (Scheme 1). The compounds are numbered **1**–**5**, in order of increasing pK_a of the parent amine.[47–50] In all cases, the β-glycoside was the major product. For compounds **1**, **2**, and **3** the α-glycoside could be isolated as a minor side product. The structural identity of isomers was identified using NMR. In comparison with the α-glycoside, the β-glycoside anomeric proton is shifted upfield (ranging from 3.9 to 4.8 ppm for the β, and 5.2 to 5.4 ppm for the α-epimer). These trends are consistent with the known assignments of [^{19}F]FDG itself (4.79 ppm for the β anomer and 5.33 ppm for the α anomer).[51] The $J_{1,2}$ coupling constant was also greater for β-glycosides (8.6 Hz, compared to 7.8 Hz for [^{19}F]FDG) than α-glycosides (5.1–5.5 Hz, compared to 3.8 Hz for ^{19}F-FDG).

As a control compound, [^{19}F]FDG benzyl oxime **6** was synthesized. In contrast with β glycosides, oximes have much greater hydrolytic stability at mildly acidic pH, such that they do not decompose on a time scale relevant for PET imaging.[52] [^{18}F]FDG has been used to label peptides via an oxime bond, and the resulting conjugates did not hydrolyze to [^{18}F]FDG to any significant extent.[35–37] This compound was synthesized in one step from [^{19}F]FDG and *O*-benzylhydroxylamine (Scheme 1B). Yields of syntheses for the [^{19}F]FDG amines and [^{19}F]FDG oxime are summarized in Table 1.

Radiosynthesis of [^{18}F]FDG Amine and [^{18}F]FDG Oxime Tracers

Radiosynthesis of [^{18}F]FDG amines and oxime was accomplished in one step from [^{18}F]FDG by incubation with the parent amine in the presence of acetic acid at 80 °C. Reaction times ranged from 1 to 30 min (see Supporting Information for full methods). All compounds were purified by reversed phase HPLC. Representative radio-HPLC traces of the

crude reactions are presented in Figure 2 and SI Figures S1–S3. All compounds were greater than 95% pure following synthesis. Radiosynthetic yields are summarized on Table 1. For [^{18}F]FDG amines, the β-glycoside was the major product in all cases, confirmed by coinjection with the ^{19}F standard (Figure 2A,B, SI Figures S4–S8). The α-glycoside was obtained as a minor side product. For [^{18}F]FDG oxime **6**, the E-oxime was the major product, confirmed by coinjection experiments (Figure 2C, SI Figure S9). The Z-oxime was obtained as a minor side product.

In Vitro Assay of FDG Amine Decomposition to FDG

We first tested if FDGamines would decompose to FDG under acidic conditions. When treated with 1 M acetic acid for 5 min, all [^{18}F]FDG amines showed significant decomposition to [^{18}F]FDG, confirmed by HPLC and TLC (SI Figures S4–S8).

We next tested the rate of decomposition of [^{18}F]FDG amines at pH 7.4, the normal interstitial pH, and pH 6.5, the mildly acidic pH typically associated with solid tumors (SI Figure S10), using an HPLC assay. All compounds were tested at 15 min (Figure 3A) and 1 h (Figure 3B). There was increased decomposition of [^{18}F]FDG amines **2**–**5** at pH 6.5 in comparison with pH 7.4. Furthermore, the overall rate of decomposition followed the pK_a of the parent amine. These results are concordant with previous studies of other glycosylamines, which also found that the rate of decomposition was accelerated at mildly acidic pH, and proportional to the pK_a of the parent amine.[46] These effects can be rationalized by the known mechanism of hydrolysis of glycosylamines, which requires protonation of the Schiff base intermediate.[46] As expected based on the known hydrolytic stability of oximes,[52] [^{18}F]FDG oxime **6** had undetectable hydrolysis at both pHs 7.4 and 6.5. These results suggested that [^{18}F]FDG amines could be hydrolyzed rapidly at acidic pH, and consequently could act as acid labile prodrugs for imaging acidic microenvironments.

Accumulation of ^{18}F in PC3 Cells Incubated with [^{18}F]FDG Amine 2 is Accelerated in Mildly Acidic Conditions

The degree of [^{18}F]FDG amine cell uptake was assessed in an in vitro model of an acidic tumor microenvironment. PC3 cells are a line originally derived from a bone metastasis of prostate cancer, which is a model of high grade, androgen independent prostate cancer.[53] PC3 cells are an optimal model for an initial proof of principle study of [^{18}F]FDG amines as acid labile prodrugs, since PC3 cells are known to have [^{18}F]FDG uptake, in cell culture and in murine xenografts.[54,55] Furthermore, PC3 xenografts are known to develop the acidic interstitial pH typical for solid tumors (average $pH_e = 6.93 \pm 0.03$).[25]

PC3 cells were incubated with either [^{18}F]FDG, [^{18}F]FDG amine **2**, or [^{18}F]FDG oxime **6** (Figure 4). Uptake of [^{18}F]FDG amine **2** was increased at pH 6.5 in comparison with pH 7.4. In contrast, the uptake of [^{18}F]FDG oxime **6** was low and unchanged at pH 7.4 and pH 6.5, and the uptake of [^{18}F]FDG was decreased at pH 6.5. The reason that [^{18}F]FDG uptake is decreased at pH 6.5 in comparison with 7.4, is unclear, but may be related to the generalized metabolic state of the cells. These results are consistent with a mechanism of uptake of [^{18}F]FDG amine **2**, which is dependent at least in part on acidic pH. We also tested if cytochalasin B, a known inhibitor of glucose and fluorodeoxyglucose uptake,[56] blocked

uptake of the radiopharmaceuticals. As expected, cytochalasin B blocked uptake of [^{18}F]FDG, and also of [^{18}F]FDG amine **2**. Similar results were obtained with the addition of glucose, a known inhibitor of [^{18}F]FDG uptake (SI Figure S11).[55] Overall, these results are consistent with a mechanism of action that requires the presence of acid for maximal cell uptake, and the same mechanism of cellular uptake as [^{18}F]FDG, requiring both glucose transporters and hexokinase phosphorylation.[57,58]

PET Imaging of [^{18}F]FDG Amines and Oxime in PC3 Xenograft Mice

The in vivo performance of [^{18}F]FDG amines was evaluated in PC3 xenograft mice. PC3 xenografts were selected as a model system for the acidic tumor environment based on prior experiments demonstrating that the tumor interstitial pH is acidic (average pH_e = 6.93 ± 0.03), and also that PC3 cells take up [^{18}F]FDG.[25,54] PET imaging was performed 3–4 weeks following implantation of PC3 xenograft tumors on the shoulder of nu/nu mice. The imaging protocol was identical to that typically performed for [^{18}F]FDG, with a static 10 min PET imaging protocol acquired 55 min after injection of tracer.

Typical PET imaging results obtained using [^{18}F]FDG are presented on Figure 5A. These results are similar to those previously reported, with high levels of uptake in the tumor, brain, and heart, and renal clearance.[54] PET imaging was initially performed using [^{18}F]FDG amines **2** and **3**, with very low uptake in tumor, likely due to low rates of hydrolysis and/ or rapid clearance kinetics (SI Figure S12). In order to increase the uptake in the tumor, we performed PET imaging using the more acid-labile derivative [^{18}F]FDG amine **4**. [^{18}F]FDG amine **4** had acceptable stability in serum, with 96.7 ± 1.0% intact at 15 min, and 78.2 ± 4.4% intact at 1 h. Following reformulation for injection, specific activity of [^{18}F]FDG amine **4** was 516 ± 137 Ci/mmol.

In comparison with [^{18}F]FDG, [^{18}F]FDG amine **4** demonstrates similar uptake in tumor, but reduced uptake in Harderian glands and heart (Figure 5B). [^{18}F]FDG amine **4** also demonstrates clearance via the hepatobiliary system as well as the renal collecting system. In contrast, [^{18}F]FDG oxime **6** demonstrates no significant uptake in tumor, heart, or brain (Figure 5C), with clearance via the hepatobiliary and renal collecting systems.

Consistent with previous results, [^{18}F]FDG shows uptake in the tumor, but a much higher degree of uptake in the heart (Figure 5A). In contrast, [^{18}F]FDG amine **4** shows a similar degree of uptake in the tumor and heart (Figure 5B). [^{18}F]FDG oxime **6** shows very low uptake in both heart and tumor (Figure 5C). We also performed biodistribution analysis of [^{18}F]FDG amine **4**. These results are compared against the previously reported biodistribution of [^{18}F]FDG in PC3 xenografts, acquired using the same experimental technique as in our study of the [^{18}F]FDG amine **4** (SI Table 2).[54] These results recapitulate the imaging experiments outlined above, as [^{18}F]FDG amine **4** demonstrates a similar level of uptake in tumor in comparison with [^{18}F]FDG (5.4 vs 3.6% i.d./g, respectively), but reduced uptake in the heart (15 vs 57% i.d./g, respectively).

These findings are consistent with a mechanism of action in which relatively greater levels of uptake of tracer is seen in acidic tissues (e.g., tumor), in comparison with less acidic

regions (muscle or heart). This may be due to a greater level of hydrolysis of [^{18}F]FDG amine to [^{18}F]FDG in acidic tissues in comparison with normal tissues (Figure 1).

Next, the uptake of [^{18}F]FDG amine was tested following alkalinization of the tumor, using previously validated models, genetic overexpression of carbonic anhydrase IX (CAIX), or pharmacologic modulation with bicarbonate. Xenografts generated from the previously described PC3-CAIX cells constitutively overexpress carbonic anhydrase IX, and form xenografts that are more alkaline in comparison with unmodified PC3 tumors. In particular, Viola-Villegas et al. found that the average interstitial pH of PC3 xenografts is 6.93 ± 0.03, and that of PC3-CAIX tumors is 7.07 ± 0.04.[25] Treatment with sodium bicarbonate has been extensively used to alkalinize the tumor microenvironment, by an average of 0.3–0.8 pH units, without significant effects on systemic pH, in several different animal models of malignancy.[6,8,59–64] Thus, PC3-CAIX and PC3 with bicarbonate treatment are well-validated models of alkalinization in previously acidic tumor xenografts.

We performed PET imaging in sodium bicarbonate treatment, PC3-CAIX, and control PC3 groups using [^{18}F]FDG, [^{18}F]FDG amine **4**, and [^{18}F]FDG oxime **6** (n = 4 animals in each group). Uptake in tissues was quantified by region of interest analysis and quantified in % injected dose per gram (Figure 6). Uptake of [^{18}F]FDG was high in tumors in both modified and unmodified PC3 xenograft mice (Figure 6A). In contrast, uptake of [^{18}F]FDG amine **4** in tumors was high in the control group but significantly reduced in the bicarbonate treatment and PC3-CAIX groups. Uptake of [^{18}F]FDG oxime **6** was very low in both control and treatment groups. Similar trends were observed when tumor:muscle uptake ratios were calculated (SI Figure S13). To verify that this effect was specific to the tumor rather than an alteration in systemic pH, uptake in muscle, heart, and tumor was compared in PC3 xenograft mice in bicarbonate treatment, PC3 CAIX, and control groups (Figure 6B). While uptake in tumor was significantly reduced by sodium bicarbonate treatment or carbonic anhydrase overexpression, uptake in heart or muscle was not. Overall, these data support a mechanism of uptake that requires interstitial acidity for full uptake of radiopharmaceutical (Figure 1).

DISCUSSION

We have presented the design of a generally applicable prodrug strategy for targeting of acidic interstitial pH. This strategy was applied to a new class of PET imaging tracers for probing the acidic interstitial tumor microenvironment. Interstitial acidity is a promising biomarker for detecting the presence of aggressive subpopulations of cancer. We have presented data showing that glycosylamines of [^{18}F]fluorodeoxyglucose, termed [^{18}F]FDG amines, are acid labile prodrugs of [^{18}F]FDG. The proposed mechanism of action of [^{18}F]FDG amine is via two-step, prodrug mechanism (Figure 1). This proposed mechanism first requires general acid catalyzed hydrolysis of the [^{18}F]FDG amine to [^{18}F]FDG. [^{18}F]FDG is then taken up in cells via glucose transporter, and trapped in the cell by phosphorylation. Since glycosylamines are in equilibrium with the parent sugar and amine, the compounds can be readily synthesized in the presence of excess amine (Scheme 1). Following dilution to tracer levels, the parent amine is present at low concentrations, and the hydrolysis reaction is favored. Notably, the rate of decomposition to [^{18}F]FDG is tunable in

a predictable manner based on the pK_a of the parent amine. [^{18}F]FDG amines were applied to an uptake assay in PC3 cells, with the key finding that uptake is increased at mildly acidic pH, and likely requires glucose transporters. Uptake of [^{18}F]FDG amine **4** in PC3 xenograft tumors was elevated relative to healthy tissue as shown by PET imaging and biodistribution experiments, whereas the control compound [^{18}F]FDG oxime **6** with no pH sensitivity exhibited relatively low uptake. Alkalinization of the tumors with sodium bicarbonate, or by overexpression of carbonic anhydrase, reduced [^{18}F]FDG amine uptake, supporting a mechanism of radiopharmaceutical uptake requiring interstitial acidity. While interstitial acidity appears to modulate probe uptake in tumor, it is likely that there is some spontaneous decomposition of the FDG amine to FDG in neutral pH tissues, potentially increasing probe uptake in nonacidic tissues. However, the serum stability results demonstrating that the probe was 78% intact at 1 h, as well as the relative decrease of uptake in the PC3 CAIX model, argue against the possibility that nontumoral hydrolysis is the major mechanism of probe uptake. Nevertheless, this represents a potential limitation of this technique, and an important area for future study.

The rate of hydrolysis of [^{18}F]FDG amines is tunable and follows the pK_a of the parent amine, consistent with prior studies, and as expected based on the known mechanism of glycosylamine hydrolysis.[46] These different rates of hydrolysis are best suited for different applications. For example, the relatively stable [^{18}F]FDG amine **2** performed well in a cell-based assay that requires 1 h incubation. In contrast, the more unstable 4-phenylbenzylamine [^{18}F]FDG amine **4** performed well in vivo. This is likely because the rapid time frame of hydrolysis coincides with rapid clearance of the radiopharmaceutical. Further experiments are necessary to determine which rate of hydrolysis is optimal for providing the best contrast to noise ratio for imaging the acidic microenvironment. In a more general sense, the concept of tunable glycosylamine linkages may find wider applicability as a prodrug strategy. For example, the more stable [^{18}F]FDG amine linkages could find application in imaging using longer-lived therapeutic isotopes or stable contrast agents, or in drug delivery. In this regard, an outstanding challenge will be to minimize side reactions such as the Amadori rearrangement, which results in glycosylamines of sugars with a hydroxyl group at the 2 position.

[^{18}F]FDG amines differ from previously reported methods for imaging acidic pH in several ways, and complement existing technologies. Magnetic resonance based techniques are the most commonly used in the field; however, these techniques have several limitations, including a relatively small field of view, low spatial resolution, low signal-to-noise ratio, requirement for administration of high doses of probe, potentially perturbing tissue pH, and requirement for specialized coils and equipment.[7,14] In contrast, [^{18}F]FDG amines are straightforward to synthesize, are administered at tracer doses, and take advantage of the good resolution of existing PET imaging technologies, which allow imaging of large fields of view. Uptake of [^{18}F]FDG amines in tumor was high (ranging from 3.5–5.4% i.d./g), which compares favorably with previously reported PET tracers for targeting the acidic environment.[22,23,25] Unlike existing PET technologies for imaging acidic interstitial pH, the uptake of [^{18}F]FDG amines requires GLUT transporter and hexokinase. While the majority of cancers do have high [^{18}F]FDG uptake, which has led to its widespread use, some do not.

Therefore, uptake of [^{18}F]FDG amines in glycolytically inactive, acidic tumors may be reduced. This represents a possible limitation of this technique, and a matter for further investigation.

Another interesting finding was that the relative uptake of [^{18}F]FDG amine **4** in tumor versus the heart was greater than that for [^{18}F]FDG. This raises the possibility that [^{18}F]FDG amines could find more general applicability in oncologic PET imaging, for targeting acidic disease in areas of normal high physiologic [^{18}F]FDG uptake, such as brain, heart, or liver. Detection of metastasis or primary tumors in these regions is limited in clinical [^{18}F]FDG PET imaging protocols due to the high background uptake of [^{18}F]FDG.[65] This question is currently under investigation in our laboratory.

EXPERIMENTAL SECTION

General Methods for Synthesis of [^{19}F]FDG Amines and Oxime

Solutions containing 0.25 M [^{19}F]FDG, 0.5 M amine, and 0.25–0.5 M acetic acid were incubated at 60 °C for 1 h with stirring. The compounds were then purified on a C18 semipreparative HPLC column and pure fractions were pooled and lyophilized. For detailed methods and characterization for each compound, see the Supporting Information.

General Methods for Synthesis of [^{18}F]FDG Amines and Oxime

[^{18}F]FDG was produced in aqueous solution using standard methods.[66] This solution was dried azeotropically using acetonitrile. 250 μL of 0.5 M solutions of the amine precursors, with 0.25–0.5 M acetic acid, were added to the residue. The resulting mixtures were incubated at 80 °C for 1–30 min, and then purified using semipreparative HPLC. Purified fractions were used directly for HPLC degradation, serum stability, and cell uptake experiments. For imaging and biodistribution experiments, compounds were reformulated into saline as follows: the HPLC eluates were diluted 1:1 with water, and loaded onto C18 Sep Pak Plus cartridges (Waters, Milford, MA). The cartridges were washed with 10 mL water, and eluted with 1 mL ethanol. The resulting eluates were dried under nitrogen stream and vacuum at room temperature to remove residual ethanol. The final products were diluted in normal saline with 10 mM sodium phosphate buffer pH 8.0 (included to minimize radiopharmaceutical decomposition prior to administration) for injection. For full experimental details, see Supporting Information.

HPLC Degradation Assay

To 200 μL of the HPLC purified compounds **1**–**6** or the indicated hydrazone derivatives was added 1.8 mL of 0.2 M sodium phosphate, at either pH 7.4 or 6.5. The mixtures were incubated at 37 °C. At 15 min and 1 h, 500 μL was injected on analytical scale C18 HPLC using the elution conditions outlined above.

Cell Uptake Studies

For cell uptake experiments, PC3 cells were seeded at a density of 4×10^5 cells per well in 12-well plates (Corning, USA) and grown at 37 °C, 5% CO_2 for 24 h. Cells were cultured at 37 °C in a 5% CO_2 incubator in the following media: RPMI 1640 medium supplemented

with 10% fetal bovine serum, 100 IU mL^{-1} penicillin, and 100 $\mu g\ mL^{-1}$ streptomycin. On the day of the experiment, cells were washed twice with ice cold PBS, followed by incubation for 3 h at 37C, 5% CO_2 in fresh free glucose medium without FBS (RPMI1640–0.5 mL per well). Thirty minutes before adding radioactive compounds, the wells were treated with cytochalasin B (CB, EMD Millipore Biosciences) dissolved in DMSO. CB is a potent reversible inhibitor of sugar uptake in cultured cells.[56] CB solutions were prepared from a stock solution of 1 mg/mL, which was stored frozen and protected from light. CB was added in order to reach a concentration of 10 mM in the cells medium. Control wells instead received the equal volume of DMSO (0.25% to 1% final DMSO concentration). Before adding radioactive compounds, the medium was removed and fresh free glucose medium without FBS with 10 mM and pH adjusted (7.4 or 6.5) was added to the cells (RPMI1640–0.5 mL per well). Viability of cells was determined by 3-[4,5-dimethylthiazol-2-yl]-2,5-diphenyl tetrazolium bromide (MTT) cell proliferation assay as described in the Supporting Information. Then 5 μCi of each radioactive compounds (FDG, FDGamine, and FDGoxime) was added for each condition. The cells were incubated at 37 °C, 5% CO_2 for 30 min. Following incubation, the cells were washed twice with ice cold PBS and retained for analysis (externalized fraction). The cells were lysed with 1 mL of 1 M NaOH and collected (cell associated fraction). The externalized and cell associated fractions were counted in a gamma counter and expressed as a percentage of the total activity added per equal relative number of cells (as determined using a MTT Cell Proliferation Assay as detailed in Supporting Information). Experiments were performed in triplicate.

Xenograft Mice

All mice were handled according to the Guide for the Care and Use of Laboratory Animals and accredited by the Association for Assessment and Accreditation of Laboratory Animal Care. Mouse studies were carried out following the procedures approved by the Laboratory Animal Resource Center facilities of UCSF. For inoculation into nude mice, PC3 cells or PC3-CAIX cells were washed with PBS, digested with trypsin, resuspended in DMEM containing fetal bovine serum, and pooled. After centrifugation, cells were resuspended in Matrigel (BD Biosciences Discovery Labware, Bedford, MA)–PBS (1:1) at a concentration of 5×10^6 cells per 100 μL. Cell/Matrigel mixture of 100 μL was injected s.c. into 6-week-old male *nu*/*nu* mice (Charles River, Wilmington, Massachusetts) on the right shoulder surface. Tumor volumes and body weights were monitored the day of the imaging experiments.

PET Imaging

All animals were fasted starting the evening before PET imaging exams to minimize muscle uptake and optimize tumor to background signal. Under isofluorane anesthesia, a tail vein catheter was placed. Between 125 and 200 μCi of [^{18}F]FDG, [^{18}F]FDGamine **4**, or [^{18}F]FDGoxime **6** was injected via the tail vein catheter. The animals were placed on a heating pad for 55 min to minimize shivering and brown fat uptake. At 1 h post-injection, the animals were transferred to a Siemens Inveon micro PET-CT system (Siemens, Erlangen, Germany), and imaged using a single static time frame of 10 min. A micro-CT scan was then obtained for attenuation correction and anatomical co-registration. No adverse events were observed during or after injection of any compound. Anesthesia was maintained during

imaging using isofluorane. All spectra were viewed using open source Amide software (amide.sourceforge.net). Quantification of uptake was performed by drawing regions of interest over indicated organs or tumor on the CT portion of the exam, and are expressed as % injected dose per gram.

Sodium Bicarbonate Treatment Protocol

At 3 weeks post-inoculation with PC3 cells, mice were split into two groups of 4 animals. One group was given sterile water, and one 200 mM sodium bicarbonate ad libitum. Imaging was performed on days 4, 5, and 6 of treatment using [^{18}F]-FDGamine 4, [^{18}F]FDG, and [^{18}F]FDGoxime 6, respectively.

Statistical Analysis

All data were analyzed in Microsoft Excel. Data were analyzed using unpaired two-tailed Student's *t* test. Differences at the 95% confidence level ($P < 0.05$) were considered to be statistically significant. All graphs are depicted with error bars corresponding to the standard error of the mean. To allow comparison with previously published results, biodistribution studies are reported ± standard deviation.

Supplementary Material

Refer to Web version on PubMed Central for supplementary material.

Acknowledgments

We gratefully acknowledge Sergio Wong for assistance with the biodistribution experiments. Human prostate cancer cell line, PC3 was a generous gift from Dr. John Cunningham, department of urology, University of California, San Francisco, USA. PC3-CAIX cell line was a generous gift of Dr. Ronald Blasberg, Memorial Sloan-Kettering Cancer Center, New York, NY. R.R.F. acknowledges support from NIH 5T32EB0011631-10, a University of California, San Francisco Department of Radiology Seed Grant, a Radiology Society of North America research fellow grant, and an SNMMI-ERF Mitzi and William Blahd, MD Pilot Grant. M.J.E. was supported by a David H. Koch Young Investigator Award from the Prostate Cancer Foundation, and NIH R00CA172695 and R01CA176671. C.J.C. thanks the NIH (GM 79465) for support. C.J.C. is an Investigator with the Howard Hughes Medical Institute. D.M.W. acknowledges support from NIH R01CA166766.

References

1. Volk T, Jahde E, Fortmeyer HP, Glusenkamp KH, Rajewsky MF. pH in human tumour xenografts: effect of intravenous administration of glucose. Br J Cancer. 1993; 68:492–500. [PubMed: 8353039]
2. Helmlinger G, Yuan F, Dellian M, Jain RK. Interstitial pH and pO2 gradients in solid tumors in vivo: high-resolution measurements reveal a lack of correlation. Nat Med. 1997; 3:177–82. [PubMed: 9018236]
3. Gatenby RA, Gillies RJ. Why do cancers have high aerobic glycolysis? Nat Rev Cancer. 2004; 4:891–9. [PubMed: 15516961]
4. Martin GR, Jain RK. Noninvasive measurement of interstitial pH profiles in normal and neoplastic tissue using fluorescence ratio imaging microscopy. Cancer Res. 1994; 54:5670–4. [PubMed: 7923215]
5. Keshari KR, Sriram R, Koelsch BL, Van Criekinge M, Wilson DM, Kurhanewicz J, Wang ZJ. Hyper-polarized 13C-pyruvate magnetic resonance reveals rapid lactate export in metastatic renal cell carcinomas. Cancer Res. 2013; 73:529–38. [PubMed: 23204238]

6. Estrella V, Chen T, Lloyd M, Wojtkowiak J, Cornnell HH, Ibrahim-Hashim A, Bailey K, Balagurunathan Y, Rothberg JM, Sloane BF, et al. Acidity generated by the tumor microenvironment drives local invasion. Cancer Res. 2013; 73:1524–35. [PubMed: 23288510]
7. Hashim AI, Zhang X, Wojtkowiak JW, Martinez GV, Gillies RJ. Imaging pH and metastasis. NMR Biomed. 2011; 24:582–91. [PubMed: 21387439]
8. Robey IF, Baggett BK, Kirkpatrick ND, Roe DJ, Dosescu J, Sloane BF, Hashim AI, Morse DL, Raghunand N, Gatenby RA, et al. Bicarbonate increases tumor pH and inhibits spontaneous metastases. Cancer Res. 2009; 69:2260–8. [PubMed: 19276390]
9. Parks SK, Chiche J, Pouyssegur J. Disrupting proton dynamics and energy metabolism for cancer therapy. Nat Rev Cancer. 2013; 13:611–23. [PubMed: 23969692]
10. Neri D, Supuran CT. Interfering with pH regulation in tumours as a therapeutic strategy. Nat Rev Drug Discovery. 2011; 10:767–77. [PubMed: 21921921]
11. Maschauer S, Prante O, Hoffmann M, Deichen JT, Kuwert T. Characterization of 18F-FDG uptake in human endothelial cells in vitro. J Nucl Med. 2004; 45:455–60. [PubMed: 15001687]
12. Binauld S, Stenzel MH. Acid-degradable polymers for drug delivery: a decade of innovation. Chem Commun (Cambridge, U K). 2013; 49:2082–102.
13. West KR, Otto S. Reversible covalent chemistry in drug delivery. Curr Drug Discovery Technol. 2005; 2:123–60.
14. Zhang X, Lin Y, Gillies RJ. Tumor pH and its measurement. J Nucl Med. 2010; 51:1167–70. [PubMed: 20660380]
15. Gillies RJ, Raghunand N, Garcia-Martin ML, Gatenby RA. pH imaging. A review of pH measurement methods and applications in cancers. IEEE engineering in medicine and biology magazine: the quarterly magazine of the Engineering in Medicine & Biology Society. 2004; 23:57–64.
16. Gillies RJ, Liu Z, Bhujwalla Z. 31P-MRS measurements of extracellular pH of tumors using 3-aminopropyl-phosphonate. Am J Physiol. 1994; 267:C195–203. [PubMed: 8048479]
17. van Sluis R, Bhujwalla ZM, Raghunand N, Ballesteros P, Alvarez J, Cerdan S, Galons JP, Gillies RJ. In vivo imaging of extracellular pH using 1H MRSI. Magn Reson Med. 1999; 41:743–50. [PubMed: 10332850]
18. Gallagher FA, Kettunen MI, Day SE, Hu DE, Ardenkjaer-Larsen JH, Zandt R, Jensen PR, Karlsson M, Golman K, Lerche MH, et al. Magnetic resonance imaging of pH in vivo using hyperpolarized 13C-labelled bicarbonate. Nature. 2008; 453:940–3. [PubMed: 18509335]
19. Flavell RR, von Morze C, Blecha JE, Korenchan DE, Van Criekinge M, Sriram R, Gordon JW, Chen HY, Subramaniam S, Bok RA, et al. Application of Good's buffers to pH imaging using hyperpolarized 13C MRI. Chem Commun. 2015; 51:14119–14122.
20. Rottenberg DA, Ginos JZ, Kearfott KJ, Junck L, Bigner DD. In vivo measurement of regional brain tissue pH using positron emission tomography. Ann Neurol. 1984; 15:S98–102. [PubMed: 6611132]
21. Rottenberg DA, Ginos JZ, Kearfott KJ, Junck L, Dhawan V, Jarden JO. In vivo measurement of brain tumor pH using [11C]DMO and positron emission tomography. Ann Neurol. 1985; 17:70–9. [PubMed: 3872621]
22. Bauwens M, De Saint-Hubert M, Cleynhens J, Brams L, Devos E, Mottaghy FM, Verbruggen A. Radio-iodinated phenylalkyl malonic acid derivatives as pH-sensitive SPECT tracers. PLoS One. 2012; 7:e38428. [PubMed: 22719886]
23. Vavere AL, Biddlecombe GB, Spees WM, Garbow JR, Wijesinghe D, Andreev OA, Engelman DM, Reshetnyak YK, Lewis JS. A novel technology for the imaging of acidic prostate tumors by positron emission tomography. Cancer Res. 2009; 69:4510–6. [PubMed: 19417132]
24. Daumar P, Wanger-Baumann CA, Pillarsetty N, Fabrizio L, Carlin SD, Andreev OA, Reshetnyak YK, Lewis JS. Efficient (18)F-labeling of large 37-amino-acid pHLIP peptide analogues and their biological evaluation. Bioconjugate Chem. 2012; 23:1557–66.
25. Viola-Villegas NT, Carlin SD, Ackerstaff E, Sevak KK, Divilov V, Serganova I, Kruchevsky N, Anderson M, Blasberg RG, Andreev OA, et al. Understanding the pharmacological properties of a metabolic PET tracer in prostate cancer. Proc Natl Acad Sci U S A. 2014; 111:7254–9. [PubMed: 24785505]

26. Lippert AR, van de Bittner GC, Chang CJ. Boronate Oxidation as a Bioorthogonal Reaction Approach for Studying the Chemistry of Hydrogen Peroxide in Living Systems. Acc Chem Res. 2011; 44:793–804. [PubMed: 21834525]
27. Carroll V, Michel BW, Blecha J, VanBrocklin H, Keshari K, Wilson D, Chang CJ. A boronate-caged [(1) (8)F]FLT probe for hydrogen peroxide detection using positron emission tomography. J Am Chem Soc. 2014; 136:14742–5. [PubMed: 25310369]
28. Fletcher JW, Djulbegovic B, Soares HP, Siegel BA, Lowe VJ, Lyman GH, Coleman RE, Wahl R, Paschold JC, Avril N, et al. Recommendations on the use of 18F-FDG PET in oncology. J Nucl Med. 2008; 49:480–508. [PubMed: 18287273]
29. Bormans G, Verbruggen A. Enzymatic synthesis and biodistribution in mice of beta-O-D-galactopyranosyl-(1,4′)-2′-[1 F-18]fluoro-2′-deoxy-D-glucopyranose (2′-[F-18]-fluorodeoxylactose). J Labelled Compd Radiopharm. 2001; 44:417–423.
30. Patt M, Sorger D, Scheunemann M, Stocklin G. Adduct of 2-[18F]FDG and 2-nitroimidazole as a putative radiotracer for the detection of hypoxia with PET: synthesis, in vitro- and in vivo-characterization. Appl Radiat Isot. 2002; 57:705–12. [PubMed: 12433045]
31. Maschauer S, Pischetsrieder M, Kuwert T, Prante O. Utility of 1,3,4,6-tetra-O-acetyl-2-deoxy-2-[F-18]-fluoroglucopyranoside for no-carrier-added F-18-glycosylation of amino acids. J Labelled Compd Radiopharm. 2005; 48:701–719.
32. Prante O, Einsiedel J, Haubner R, Gmeiner P, Wester HJ, Kuwert T, Maschauer S. 3,4,6-tri-O-acetyl-2-deoxy-2-[F-18]fluoroglucopyranosyl phenylthiosulfonate: A thiol-reactive agent for the chemoselective F-18-glycosylation of peptides. Bioconjugate Chem. 2007; 18:254–262.
33. Prante O, Hamacher K, Coenen HH. Chemoenzymatic n. c.a synthesis of the coenzyme UDP-2-deoxy-2-(F-18)fluoro-alpha-D-glucopyranose as substrate of glycosyltransferases. J Labelled Compd Radiopharm. 2007; 50:55–63.
34. Wuest F, Berndt M, Bergmann R, van den Hoff J, Pietzsch J. Synthesis and application of [(18)F]FDG-maleimidehexyloxime ([(18)F]FDG-MHO): A [(18)F]FDG-based prosthetic group for the chemoselective (18)F-labeling of peptides and proteins. Bioconjugate Chem. 2008; 19:1202–1210.
35. Wuest F, Hultsch C, Berndt M, Bergmann R. Direct labelling of peptides with 2-[18F]fluoro-2-deoxy-d-glucose ([18F]FDG). Bioorg Med Chem Lett. 2009; 19:5426–8. [PubMed: 19665892]
36. Hultsch C, Schottelius M, Auernheimer J, Alke A, Wester HJ. (18)F-Fluoroglucosylation of peptides, exemplified on cyclo(RGDfK). Eur J Nucl Med Mol Imaging. 2009; 36:1469–74. [PubMed: 19350236]
37. Namavari M, Cheng Z, Zhang R, De A, Levi J, Hoerner JK, Yaghoubi SS, Syud FA, Gambhir SS. A novel method for direct site-specific radiolabeling of peptides using [18F]FDG. Bioconjugate Chem. 2009; 20:432–6.
38. Flavell RR, Kothari P, Reed B, Vallabhajosula S, Goldsmith S, Muir TW, Kreek MJ. Rapid F-18 labeling of peptides using aniline catalyzed oximation with [18F]FDG. J Nucl Med. 2011; 52(Supplement 1):1498.
39. Baranwal A, Patel HH, Mukherjee J. 18F-Fluorodeoxyglycosylamines: Maillard reaction of 18F-fluorodeoxyglucose with biological amines. J Labelled Compd Radiopharm. 2014; 57:86–91.
40. Gudmundsdottir AV, Nitz M. Hydrolysis rates of 1-glucosyl-2-benzoylhydrazines in aqueous solution. Carbohydr Res. 2007; 342:749–752. [PubMed: 17239357]
41. Isbell HS, Frush HL. Effect of pH in the mutarotation and hydrolysis of glycosylamines. J Am Chem Soc. 1950; 72:1043–1044.
42. Isbell HS, Frush HL. Mechanisms for the Mutarotation and Hydrolysis of the Glycosylamines and the Mutarotation of the Sugars. J Research Natl Bur Standards. 1951; 46:132–144.
43. Isbell HS, Frush HL. Mutarotation, Hydrolysis, and Rearrangement Reactions of Glycosylamines. J Org Chem. 1958; 23:1309–1319.
44. Bridiau N, Benmansour M, Legoy MD, Maugard T. One-pot stereoselective synthesis of beta-N-aryl-glycosides by N-glycosylation of aromatic amines: application to the synthesis of tumor-associated carbohydrate antigen building blocks. Tetrahedron. 2007; 63:4178–4183.
45. Hellwig M, Henle T. Baking, ageing, diabetes: a short history of the Maillard reaction. Angew Chem, Int Ed. 2014; 53:10316–29.

46. Capon B, Connett BE. Mechanism of Hydrolysis of N-Aryl-D-Glucosylamines. J Chem Soc. 1965:4497–4502.

47. Haynes, WM., editor. CRC Handbook of Chemistry and Physics. 94. CRC Press; 2013.

48. Braude EA, Nachod FC. Determination of organic structures by physical methods. 1955; 6

49. Mollin J, Kasparek F, Lasovsky J. On the basicity of hydroxylamine and its derivatives. Chemicke Zvesti. 1975; 1:39–43.

50.

The pK_a of 4-phenylbenzylamine was calculated using ACD Labs version 12.

51. Fokt I, Szymanski S, Skora S, Cybulski M, Madden T, Priebe W. D-glucose- and D-mannose-based antimetabolites. Part 2 Facile synthesis of 2-deoxy-2-halo-D-glucoses and -D-mannoses. Carbohydr Res. 2009; 344:1464–73. [PubMed: 19625015]

52. Kalia J, Raines RT. Hydrolytic stability of hydrazones and oximes. Angew Chem, Int Ed. 2008; 47:7523–6.

53. Kaighn ME, Narayan KS, Ohnuki Y, Lechner JF, Jones LW. Establishment and Characterization of a Human Prostatic-Carcinoma Cell-Line (Pc-3). Invest Urol. 1979; 17:16–23. [PubMed: 447482]

54. Andersen KF, Divilov V, Koziorowski J, Pillarsetty N, Lewis JS. Antilipolytic drug boosts glucose metabolism in prostate cancer. Nucl Med Biol. 2013; 40:524–8. [PubMed: 23454248]

55. Andersen KF, Divilov V, Sevak K, Koziorowski J, Lewis JS, Pillarsetty N. Influence of free fatty acids on glucose uptake in prostate cancer cells. Nucl Med Biol. 2014; 41:254–8. [PubMed: 24440212]

56. Kletzien RF, Perdue JF, Springer A. Cytochalasin A and B. Inhibition of sugar uptake in cultured cells. J Biol Chem. 1972; 247:2964–6. [PubMed: 4337109]

57. Ong LC, Jin Y, Song IC, Yu S, Zhang K, Chow PKH. 2-[18F]-2-Deoxy-D-Glucose (FDG) Uptake in Human Tumor Cells is Related to the Expression of GLUT-1 and Hexokinase II. Acta Radiol. 2008; 49:1145–1153. [PubMed: 18979289]

58. Oehr P, Ruhlmann J, Kozak B, Brock H, Thieme D, Rink H. Inhibition of F-18-FDG uptake in glioblastoma cells by FDG and glucose. Acta Medica Austriaca. 1999; 26:101–103. [PubMed: 10520378]

59. Raghunand N, He X, van Sluis R, Mahoney B, Baggett B, Taylor CW, Paine-Murrieta G, Roe D, Bhujwalla ZM, Gillies RJ. Enhancement of chemotherapy by manipulation of tumour pH. Br J Cancer. 1999; 80:1005–1011. [PubMed: 10362108]

60. Robey IF, Nesbit LA. Investigating mechanisms of alkalinization for reducing primary breast tumor invasion. BioMed Res Int. 2013; 2013:485196. [PubMed: 23936808]

61. Robey IF, Martin NK. Bicarbonate and dichloroacetate: evaluating pH altering therapies in a mouse model for metastatic breast cancer. BMC Cancer. 2011; 11:235. [PubMed: 21663677]

62. Raghunand N, Mahoney BP, Gillies RJ. Tumor acidity, ion trapping and chemotherapeutics. II pH-dependent partition coefficients predict importance of ion trapping on pharmacokinetics of weakly basic chemotherapeutic agents. Biochem Pharmacol. 2003; 66:1219–29. [PubMed: 14505801]

63. Ibrahim-Hashim A, Cornnell HH, Abrahams D, Lloyd M, Bui M, Gillies RJ, Gatenby RA. Systemic buffers inhibit carcinogenesis in TRAMP mice. J Urol. 2012; 188:624–31. [PubMed: 22704445]

64. Silva AS, Yunes JA, Gillies RJ, Gatenby RA. The potential role of systemic buffers in reducing intratumoral extracellular pH and acid-mediated invasion. Cancer Res. 2009; 69:2677–84. [PubMed: 19276380]

65. Kitajima K, Nakamoto Y, Okizuka H, Onishi Y, Senda M, Suganuma N, Sugimura K. Accuracy of whole-body FDG-PET/CT for detecting brain metastases from non-central nervous system tumors. Ann Nucl Med. 2008; 22:595–602. [PubMed: 18756362]

66. Hamacher K, Coenen HH, Stocklin G. Efficient stereospecific synthesis of no-carrier-added 2-[18F]-fluoro-2-deoxy-D-glucose using aminopolyether supported nucleophilic substitution. J Nucl Med. 1986; 27:235–8. [PubMed: 3712040]

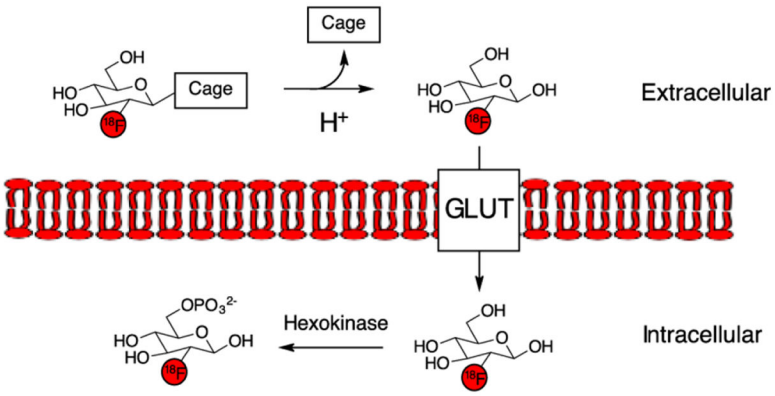

Figure 1.

Design of acid labile caged [^{18}F]FDG derivative. The mechanism of action requires loss of the acid labile protecting group, and subsequent uptake and cell trapping via GLUT transporters and hexokinase.

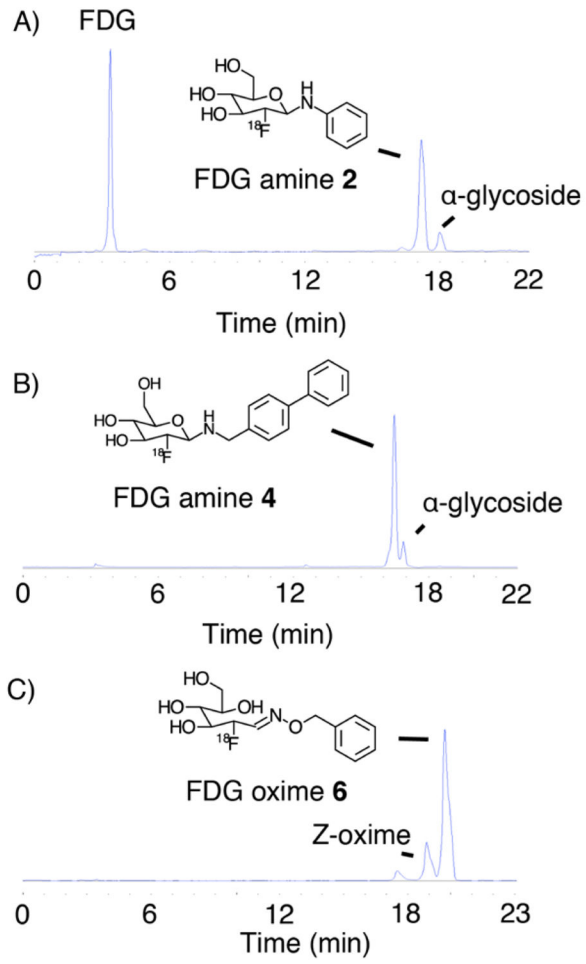

Figure 2.
Radio-HPLC of crude [^{18}F]FDG amine **2** (A), [^{18}F]FDG amine **4** (B), and [^{18}F]FDG oxime **6** (C).

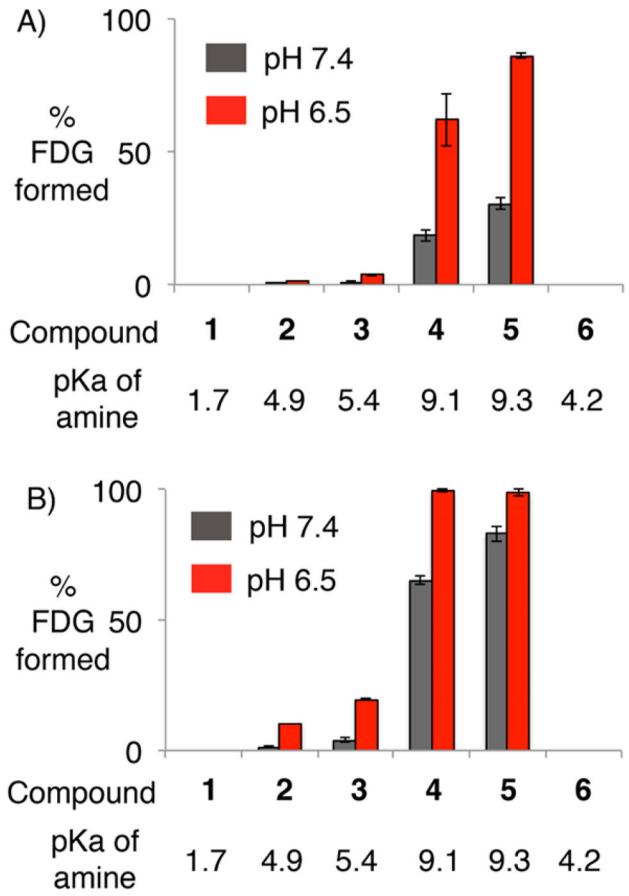

Figure 3.

HPLC assay of [^{18}F]FDG amine and oxime decomposition to [^{18}F]FDG following 15 min (A) or 1 h (B) of incubation at the indicated pH.

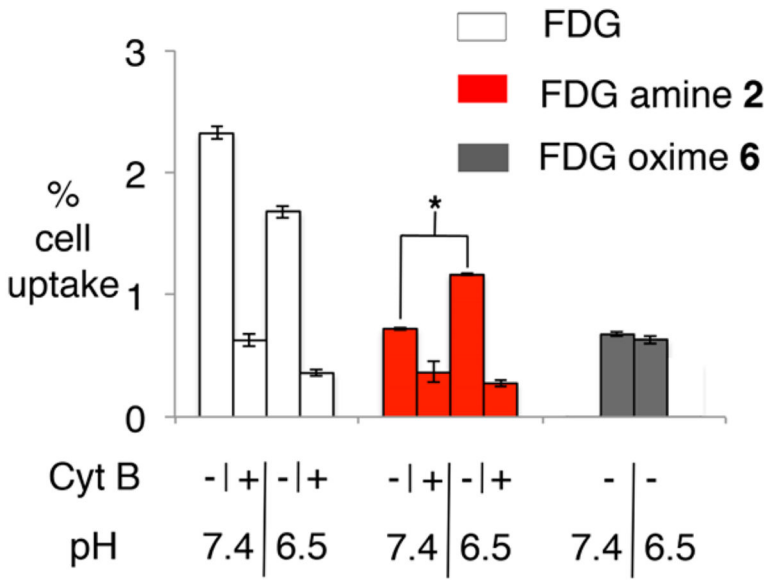

Figure 4.

PC3 cell uptake assay. Uptake of [^{18}F]FDG amine **2** is increased at pH 6.5, while uptake of [^{18}F]FDG and [^{18}F]FDG oxime **6** is not. Cell uptake was normalized to the number of viable cells, and is expressed as % cell uptake over 10^6 cells. * denotes that the difference is statistically significant with a p value <0.01.

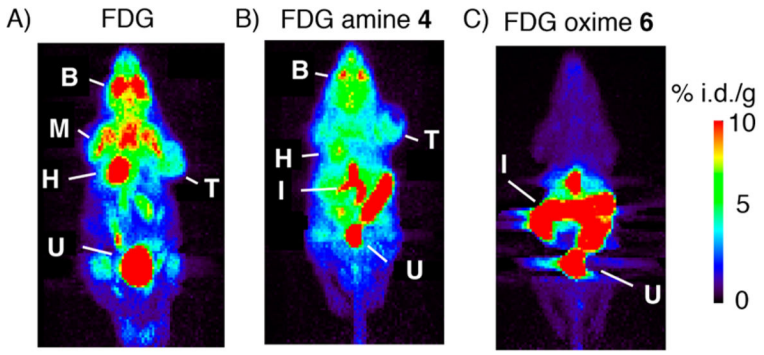

Figure 5.

PET imaging of mice with implanted PC3 xenograft tumors. Coronal maximum intensity projections following imaging with [^{18}F]FDG (A), [^{18}F]FDG amine 4 (B), or [^{18}F]FDG oxime **6** (C). All images are to the same scale as indicated. B = brain and harderian glands, M = muscle and brown fat, H = heart, T = tumor, U = Urinary bladder, I = Intestines and gallbladder, % i.d./g = percent injected dose per gram.

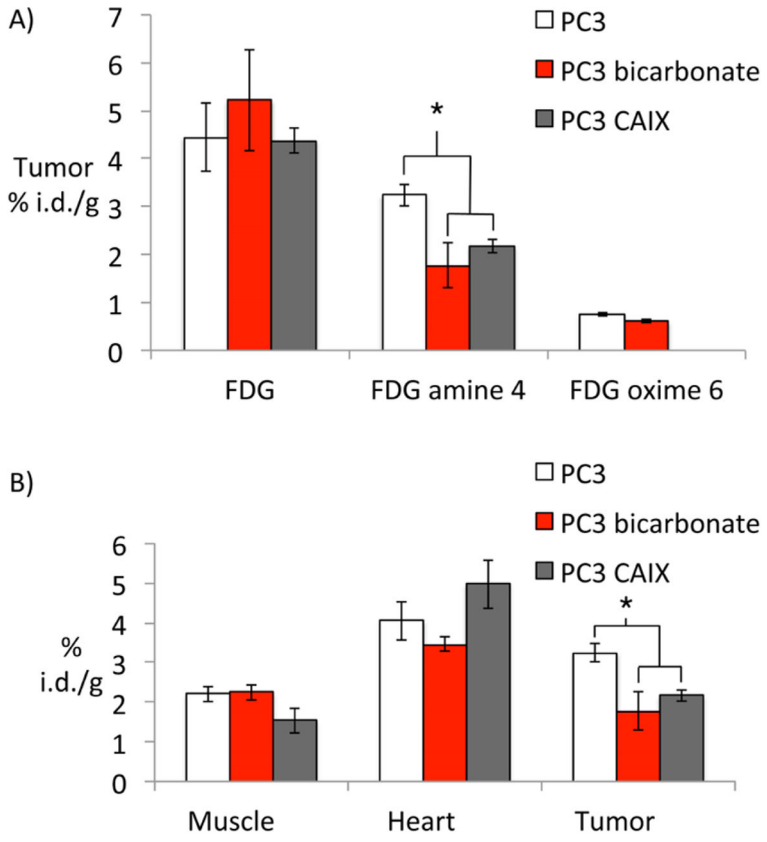

Figure 6.

Uptake of [^{18}F]FDG amine **4** is inhibited by alkalinization of the tumor in PC3 xenografts. Following PET imaging, regions of interest were drawn over the indicated organs, and the maximum uptake in each region recorded. (A) Uptake in PC3 xenograft tumors following imaging with [^{18}F]FDG, [^{18}F]FDG amine **4**, or [^{18}F]FDG oxime **6**. (B) Uptake of [^{18}F]FDG amine **4** in various organs in PC3 xenograft mice, with or without sodium bicarbonate treatment or CAIX modification. * denotes a statistically significant difference, with $p < 0.05$. Other comparisons were not statistically significant. Data are expressed as % injected dose per g (% i.d./g).

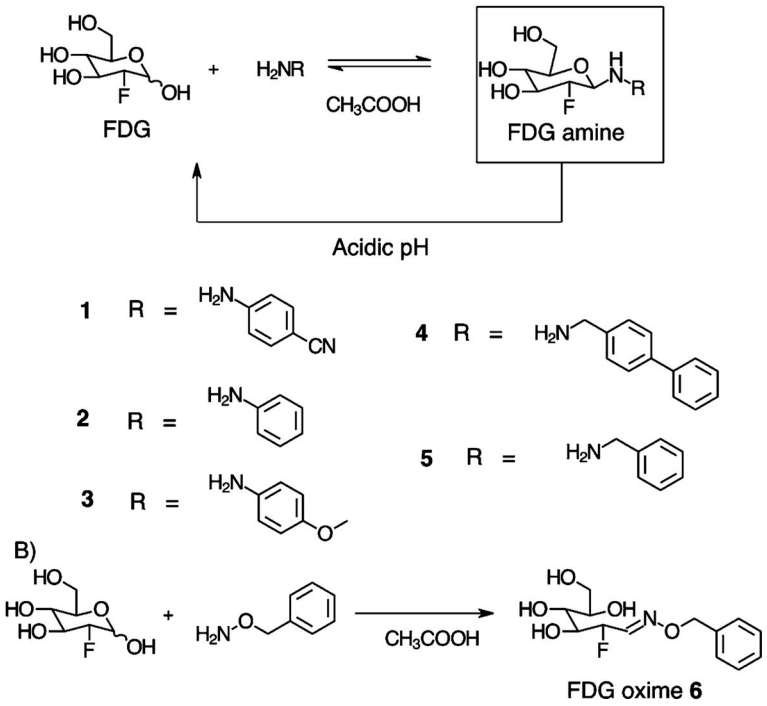

Scheme 1. (A) Synthesis of FDG Amines in One Step from FDG (either ^{18}F or ^{19}F).[a] (B) Synthesis of FDG Oxime in One Step from FDG (either ^{18}F or ^{19}F)

[a]Following treatment with acid, FDG amines decompose to form FDG.

Table 1

Summary of Synthetic Yields for [^{18}F] and [^{19}F]FDG Amines and Oximes

compound	yield of [^{19}F] product[a]	yield of [^{18}F] product[b]
1	28%	22 ± 1.3% (*n* = 3)
2	53%	37 ± 2.8% (*n* = 5)
3	50%	53 ± 0.4% (*n* = 5)
4	42%	74 ± 6.6% (*n* = 10)
5	33%	49 ± 6.4% (*n* = 10)
6	63%	75 ± 1.6% (*n* = 3)

[a] Isolated yield.

[b] Based on integration of HPLC peaks.